

Models Got Talent: Identifying High Performing Wearable Human Activity Recognition Models Without Training

Richard Goldman, Varun Komperla, Thomas Plötz, Harish Haresamudram

Georgia Institute of Technology

Atlanta, USA

{rgoldman8, vkomperla3, thomas.ploetz, harishkashyap}@gatech.edu

Abstract—Discovering high performing model architectures for wearables-based Human Activity Recognition (HAR) applications is challenging. The astonishing diversity and variability due to differing sensor locations, recording apparatus, activities etc., can cause established baseline architectures to perform worse on datasets/tasks they were not originally trained on. A promising alternative to the computationally expensive Neural Architecture Search (NAS) involves the development of *Zero Cost Proxies* (ZCPs), which correlate well with trained performance, but can be computed through a single forward/backward pass on a randomly sampled batch of data. In this paper, we investigate the effectiveness of ZCPs for HAR on six benchmark datasets, and demonstrate that they discover network architectures that obtain within 5% of performance attained by full-scale training involving 1500 randomly sampled architectures. This results in substantial computational savings as high-performing architectures can be discovered with minimal training. Our experiments not only introduce ZCPs to sensor-based HAR, but also demonstrate that they are robust to data noise, further showcasing their suitability for practical scenarios.

Index Terms—human activity recognition, zero cost proxy, wearable, mobile and ubiquitous computing

I. INTRODUCTION

A core challenge in sensor-based Human Activity Recognition (HAR) lies in identifying suitable architectures, especially if the target dataset is brand-new. Unlike other domains such as computer vision, there exists substantial diversity in wearable data, due to factors such as sensor locations, activities, participant idiosyncrasies and usage patterns [1]. Furthermore, hardware constraints as well as data and signal processing result in vastly differing data distributions, even if other recording conditions are the same. While baseline architectures are a good starting point, they may perform poorly on newly collected datasets, where there can be different and varying conditions.

Simple but effective approaches for tackling this challenge include grid search and random search, where a number of networks are trained fully to determine good architectures. Generally speaking, performing random architecture search on a much smaller subset of the grid search can be very effective, at a fraction of the computational cost [2]. Alternatively, Neural Architecture Search (NAS) algorithms discover the best architectures, but are often rather costly from a computational standpoint [3]–[5].

Another approach, which is surprisingly effective, involves developing proxy scores for network performance while using minimal data, e.g., a single minibatch of data and a single forward/backward propagation pass. Such scores are expected to be strongly correlated to performance obtained after completing training [5]. Consequently, only the top predicted network architecture(s) need to be used for full training, leading to dramatic compute and time savings relative to full grid search or other NAS methods. These efficient training-free heuristics are called ‘*Zero Cost Proxies*’ (ZCP) and are effective on common vision datasets such as CIFAR-100 [6] and subsets of ImageNet [7], but show more mixed performance for natural language and speech tasks [5]. As such, they remain underexplored for non-speech time-series data in general, and specifically for wearable sensor data.

Given the aforementioned challenge inherent to sensor-based HAR, such proxies, if effective, can be highly valuable for identifying high-performing network architectures for newly collected datasets (and more broadly, other wearable sensing applications), without expending full fledged modeling efforts. Consequently, we evaluate the *potential and effectiveness of ZCP for sensor-based HAR*.

We randomly sample 1500 convolutional and recurrent architectures, and rank them using state-of-the-art ZCPs such as `synflow`, `synflow_bn`, `jacob_cov`, `snip`, `grasp`, `fisher`, `grad_norm`, for six diverse benchmark HAR datasets. We compute the difference between the performance of the best predicted network (i.e., rank=1) and the best network obtained after training the full set of 1500 models, for each dataset and ZCP. Across datasets, the best performing ZCP have difference less than 5%, demonstrating the capability to predict HAR performance without any training. Training the top 10 predicted models further reduces the difference down to less than 1%, presenting substantial computational savings. Furthermore, ZCPs also exhibit strong rank correlation to HAR performance for three datasets, indicating their usefulness.

Given their effectiveness, we further test the ZCPs to assess their performance in practical conditions involving the presence of data noise. We observe little to no impact, clearly establishing the utility of ZCP for the development and deployment of HAR systems.

Clearly, ZCP scores are an excellent new tool for researchers

and practitioners in the community to incorporate into existing development workflows.

In summary, the contributions of this work are: (i) To the best of our knowledge, this is the first work to investigate the potential and utility of ZCP scores for sensor-based HAR; (ii) Through extensive experimental evaluation on six diverse datasets, we establish the surprising effectiveness of ZCP to score and predict HAR network performance, while using as little as a single batch of data; and (iii) We demonstrate that ZCP are robust to data noise, showcasing their practical utility for deployment scenarios.

II. RELATED WORK

A characteristic feature of wearable applications, including HAR, is wide variety in data collection protocols, human demographics, activities, and hardware, all of which result in substantial diversity in the data collected [1]. Developing suitable classifiers is therefore challenging, as established architectures perform poorly on newly collected datasets or for new application scenarios. As such, performing grid search or random search is generally effective. However, random search is more computationally efficient [2], [8], and is used as a baseline in this paper.

Neural Architecture Search (NAS) was first introduced in [9], and has been employed in computer vision for architecture discovery. A recurrent neural network (RNN) is utilized for generating classifier architectures which are then trained and provide feedback to update the RNN. However, it is accompanied by *substantial computational costs* [8]. Beyond vision tasks, its suitability for generic time-series data was evaluated in [10].

NAS has also been explored for sensor-based HAR, through Q-learning [11] and evolutionary algorithms [12], [13]. For example, [14] found that pruning search algorithms were effective in finding lightweight models on three HAR datasets. Similarly, [12] achieved high performance and low FLOPS while applying an evolutionary search algorithm to the Opportunity dataset [15], whereas [11] found success using predictions from early epochs to speed up convergence of an RL-based NAS search algorithm.

Many works also seek to discover useful architectures that suit the resource constraints of wearable applications [16], [17], and are generally referred to as μ NAS. Alternatively, randomly sampling architectures is a robust baseline, and computationally more efficient [2], [8]. Consequently, in this work, we compare the performance of ZCPs against random search.

Interest in *performance estimation* first gained momentum starting with the work of Mellor *et al.* [18], who coined the term “Zero Cost Proxy” (ZCP). It refers to techniques which require no (or minimal) upfront training to make predictions about performance obtained after full training. Since then, numerous ZCPs have been introduced. For example, [19] evaluates 28 such proxies, and [20] provides an excellent overview, categorizing them as: Jacobian-based, pruning-based, baseline, piecewise-linear, and Hessian-based. The rank correlation between the architectures ranked via ZCP and full training are

TABLE I: Architecture parameter ranges for CNN and RNN HAR networks.

Parameter	CNN	LSTM
# Layers	1 – 7	2 – 4
Out channels / Hidden size	8 – 1024 (step 8)	8 – 504 (step 8)
Kernel size	2 – 9	–
Stride	1 (fixed)	–
Dropout rate	0.1 – 0.5	0.1 – 0.5*
Total architectures	$\approx 9.23 \times 10^{25}$	$\approx 1.98 \times 10^9$

* Last LSTM layer dropout fixed at 0.0.

TABLE II: Summary of the datasets used in our evaluation.

Dataset	# Locations	# Users	# Activities
HHAR	1	9	6
Mobiact	1	61	11
Motionsense	1	24	6
Myogym	1	10	31
PAMAP2	3	9	12
RWHAR	5	15	8

used as the primary evaluation metric. In this paper, our goal is to evaluate the potential and efficacy of zero-cost proxies for predicting good architectures in the HAR domain. In addition, as our aim is to identify high performing architectures, we look beyond correlation and consider the difference in performance between the top predicted and best trained models.

III. ZERO COST PROXIES FOR HAR

The goal of this paper is to investigate the potential of zero cost proxies for identifying high performance HAR architectures. The experimental workflow for this exploration is detailed in Fig. 1 and comprises four steps: (i) Randomized architecture generation; (ii) Computation of zero cost proxies; (iii) Orchestration of full scale model training; and (iv) Performance evaluation of the ZCPs. First, we randomly sample 1500 candidate networks comprising convolutional and recurrent networks. Then, we compute the ZCPs for each dataset, generally using a single batch of data except for synflow. Subsequently, we fully train all 1500 networks and evaluate if ZCP can identify high performing networks. In what follows, we describe these steps in detail.

A. Sampling Random Architectures

We randomly sample from a broad landscape of architectures for CNN and RNN models commonly used in HAR tasks. The parameter ranges for the sampling are detailed in Table I. Among architecture parameter options, we consider key architecture variables. The CNNs contain blocks, each comprising of a 1D convolution layer, ReLU activation [21] and dropout [22]. For CNNs, we focus on: (i) the number of layers; (ii) the number of filters; (iii) the kernel size; and (iv) the dropout rate. This results in $\sim 9 \times 10^{25}$ possible architectures. In the case of RNNs, we vary: (i) the number of layers; (ii) the hidden size; and (iii) the dropout rate, resulting in $\sim 1.9 \times 10^9$ combinations. From all possible candidates, we sample 1500 architectures, at a 3:1 ratio for CNNs:RNNs, to account for the larger sample size of CNNs.

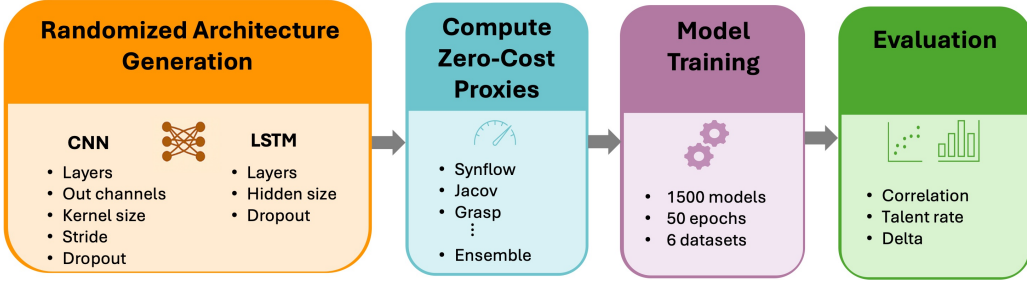


Fig. 1: The experimental pipeline contains four steps: random architecture generation, computation of the ZCPs, full training of the sampled architectures, and evaluation of the ZCPs.

B. Zero Cost Proxies

We investigate the effectiveness of eight proxies which represent a broad spectrum of techniques including Jacobian-based schemes, synaptic saliency, and simple metrics. We refer the reader to [5] for a detailed overview of the techniques, and summarize them in what follows:

a) Gradient-based: These extract clues to a model’s trainability via gradients. `jacob_cov` [18] leverages the idea that the transformation of data points by a network can be modeled using the Jacobian of the activations. In principle, the more identical the Jacobian of two data points at the start, the more difficult it will be for the network to learn to differentiate these two points. As such, the correlation of the Jacobians is used as the metric to score models. Building on ideas from the `jacob_cov` score, Abdelfattah *et al.* [5] introduced a simpler ZCP called `grad_norm`, which scores models by the Frobenius norm of their gradients.

b) Pruning-based: The Lottery Ticket Hypothesis (LTH) [23] showed that high accuracy sparse models known as "lottery-tickets" could be found via pruning and re-training. Insights on saliency pioneered in LTH were later used to discover pruning-at-initialization methods. Therein, each connection is scored using a saliency criterion and ranked according to this score. The lowest-scoring connections are removed until a desired level of network compression is reached. Abdelfattah *et al.* [5] showed that these pruning scores could be aggregated to provide information on the functionality of network as a whole relative to other networks. `snip` [24], `grasp` [25], and most recently, `synflow` [26] are all based on the idea of measuring the efficacy of the connections within a network. `snip` (Single-shot Network Pruning) approximates the change in loss observed when specific parameters are removed. `grasp` takes this a step further by computing the Hessian of loss with respect to the weights to account for the second-order effects of removing a single connection on other connections. Unlike the former two proxies, `synflow` avoids using any data altogether and relies solely on computing gradients with respect to the parameters. In this way, `synflow` is dataset agnostic and will rank models identically across datasets. `fisher` [27] measures connection saliency by using the fisher information to rank the importance of various components to a network. [5] converted this to a zero-cost proxy for any network by aggregating it

over all layers of the network. Instead of taking the loss with respect to a single pass of the data, a loss function is computed as the product of all the weights in the network.

In addition, we evaluate `plain`, which is the sum of the gradients for each weight [5]. We also investigate if the performance of the networks before any training is a good predictor of final performance. We posit that a network architecture (with random initialization) able to discriminate well between activities, will also do so after training is complete. Consequently, we utilize the validation F1-score before any training as another ZCP, and label it as `initial_val_f1`. Finally, we create an `ensemble` of all ZCPs, potentially leading to more robust predictions across datasets. It is computed as the mean of each ZCP.

C. Evaluation Metrics

We gauge the performance of the zero cost proxies using three metrics, which, put together, are good indicators of the practical utility of ZCP:

- 1) **Difference between performance of the top ranked ZCP model and the best performing model obtained after full training (Δ_1):** from a practical standpoint, the goal is to obtain the highest possible HAR performance with minimal training. Consequently, it is important to have a notion of how much the top predicted model diverges in performance from the best performing model obtained after training the full set of 1500 randomly sampled architectures. As such, lower Δ_1 indicates better the performance for the ZCPs.
- 2) **Spearman rank correlation:** it measures the overall agreement between the ranks of the models ordered using ZCPs and post-training validation performance. High correlation indicates that ZCPs can accurately predict network performance.
- 3) **Talent Rate:** the correlation scores on their own do not necessarily indicate that the best architecture will be predicted. For example, the order of the top performing models can be incorrect, while retaining high correlation due to accurate prediction on lower ranked models. Instead, we propose ‘Talent Rate’, which is defined as the percentage of architectures in the top 10% of predicted runs that are also in the top 10% of fully trained model

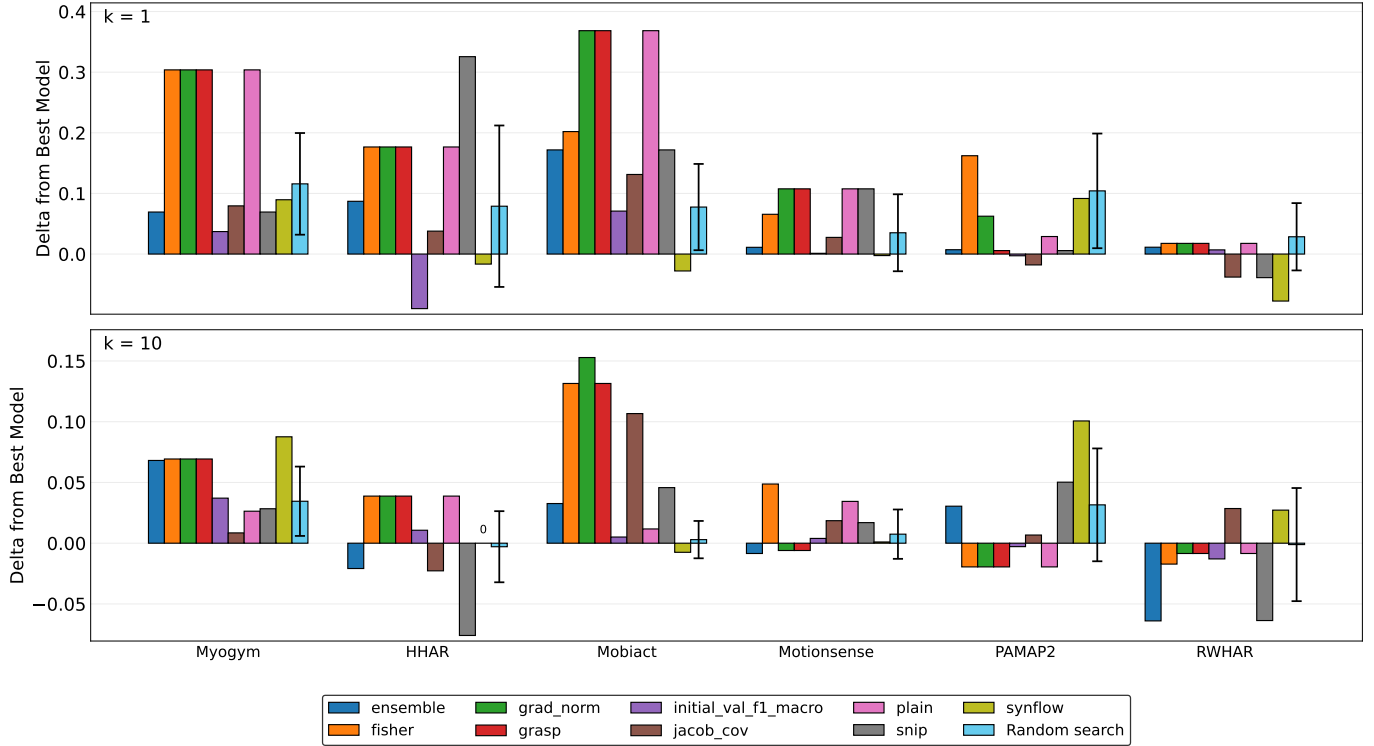


Fig. 2: Visualizing the Δ_1 and Δ_{10} : for most datasets, the difference in performance between the top predicted model and best trained model is less than 5%. However, training the top 10 predicted models reduces the difference to 1% for some ZCPs.

performances. This indicates, more broadly, whether the ZCP scores can identify good models overall. Naturally, high talent rates are better; and talent rate can be high even as correlation is relatively low.

IV. EXPERIMENTAL SETTINGS

In what follows, we detail the datasets utilized in our evaluation, along with the data pre-processing and dataset splitting strategy, and parameters such as the sampling frequency.

a) Datasets: We evaluate on *six* diverse datasets in total, chosen to cover a broad spectrum of activities, sensors, sensing locations, and number of participants. They include: (i) HHAR [1]; (ii) Mobiact [28]; (iii) Motionsense [29]; (iv) Myogym [30]; (v) PAMAP2 [31]; and (vi) RealWorld [32]. We utilize the accelerometer data only in these datasets. For HHAR, we utilize the smartwatch data, whereas Mobiact and Motionsense are recorded from a mobile phone near the waist / in the pockets. PAMAP2 has three sensing locations, including the wrist, chest, and the ankle. On the other hand, the RealWorld has seven locations – head, chest, upper arm, waist, forearm, thigh, and shin.

The datasets broadly contain locomotion style activities such as sitting, walking, standing, going up/down the stairs etc. They also have some additional activities such as biking (HHAR, MHEALTH), jumping (RealWorld, PAMAP2). There are also daily living activities such as vacuum cleaning and ironing in PAMAP2. In addition, Mobiact contains transition-style activities. Myogym is highly imbalanced (null class >75%)

and comprises fine-grained gym activities. A summary of the datasets is shown in Table II.

b) Data Pre-Processing: All datasets are separated into train-val-test splits by user IDs. First, 20% of the users are randomly chosen to comprise the test set. Of the remaining users, 20% are once again sampled randomly for validation. The rest are used for training.

The data are downsampled to 50 Hz (if the sampling rate is higher) to match the lowest frequency across all datasets. Sensor data in each split are concatenated and sliding window based segmentation with a window size of 2 seconds and overlap of 50% between segments.

c) Training Settings: All models are initialized using Xavier normal, and trained for 50 epochs using the Adam optimizer [33]. The learning rate and batch size are set to 0.0001 and 256 respectively, following prior work [34]. The learning rate is decayed by a factor of 0.8 every 10 epochs.

d) HAR Performance Evaluation Metric: We utilize the mean or macro F1-score to measure HAR performance, as it is robust to class imbalance that is often present in sensor datasets [35].

V. RESULTS

Here, we evaluate the feasibility and potential of Zero Cost Proxy ZCP) scores for sensor-based HAR, by studying (i) the Δ_1 ; (ii) the talent rate for discovering high performing models; and (iii) the ability of ZCP to rank model performance, as measured using Spearman rank correlation.

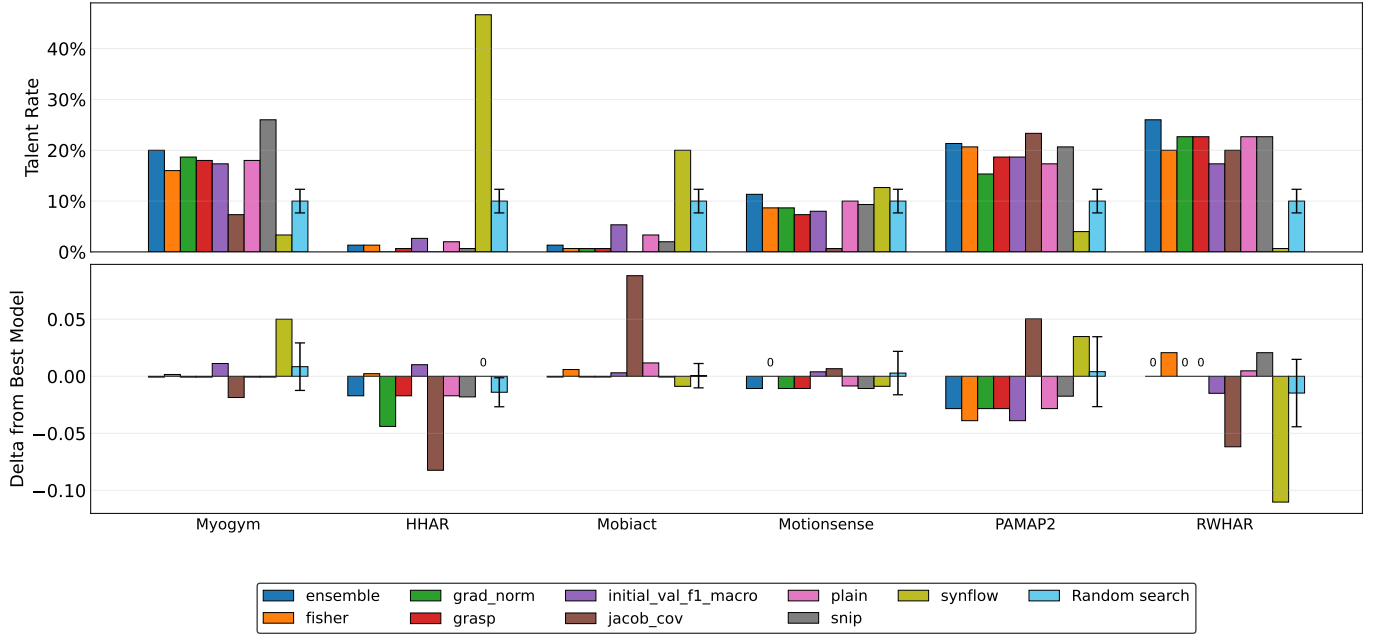


Fig. 3: Visualizing the talent rate and Δ for top 10% of predicted models: for most datasets, difference in performance between the best predicted model and those recognized after full scale training are less than 2%.

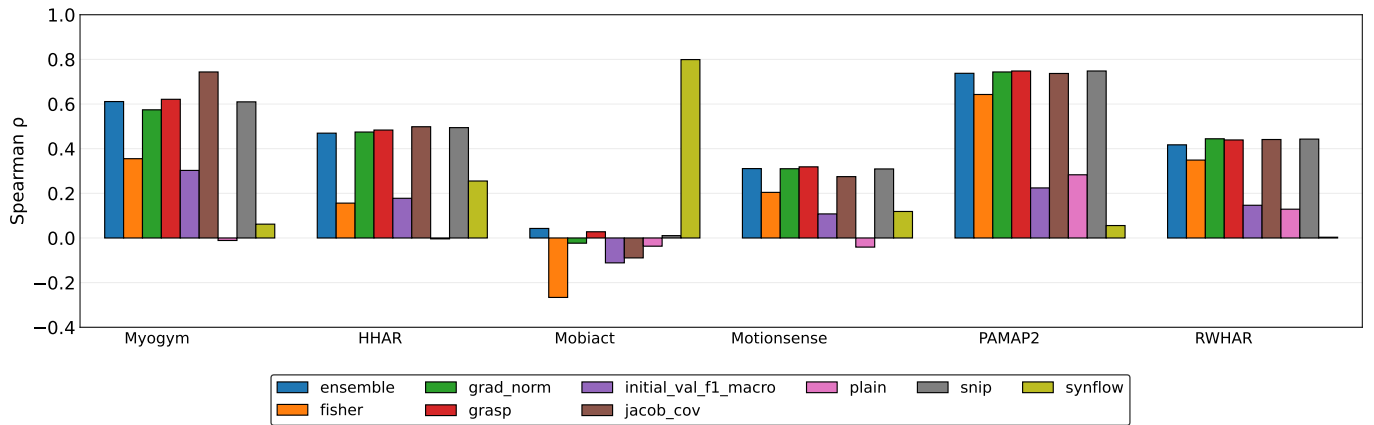


Fig. 4: Spearman rank correlation between the models ranked by ZCP and full training.

A. Difference between performance of best predicted model and best fully trained model (Δ_1)

The utility of ZCPs lies in their ability to discover high performing HAR architectures through minimal training. Consequently, a critical measure of success is the difference in performance between the best model predicted by ZCPs and those identified after fully training the entire set of 1500 architectures (denoted as Δ_1). The closer Δ_1 is to zero, the better is the performance of the ZCP, as it would mean that the best performing architectures can be identified at close to zero (or minimal) cost.

In Fig. 2 (top), we visualize the Δ_1 for each dataset and ZCP. For most datasets, the *best performing ZCP measures have $\Delta_1 < 5\%$* , indicating their *practical utility* in the wearables

domain, as newly collected datasets or novel tasks can be effectively tackled using ZCP. For PAMAP2, *grasp* has $\Delta_1 < 1\%$, i.e., it can essentially identify the best architecture, whereas for RWHAR, it is around 8%.

Interestingly, ZCP are less effective for single-sensor datasets, e.g., HHAR, Mobiact, and Myogym, than for the multi-sensor datasets such as PAMAP2 and RWHAR. Further, we also observe that the difference is negative for some datasets, e.g., HHAR, Mobiact, and RWHAR. This indicates that the corresponding zero cost proxies led to higher test set performance than the full scale training, which involves choosing the best model based on the validation F1-score. While ZCP measures such as *fisher*, *initial_val_f1_score*, and *grad_norm* are broadly effective, the *ensemble* of ZCP scores allows us to utilize all available measures (see Section III

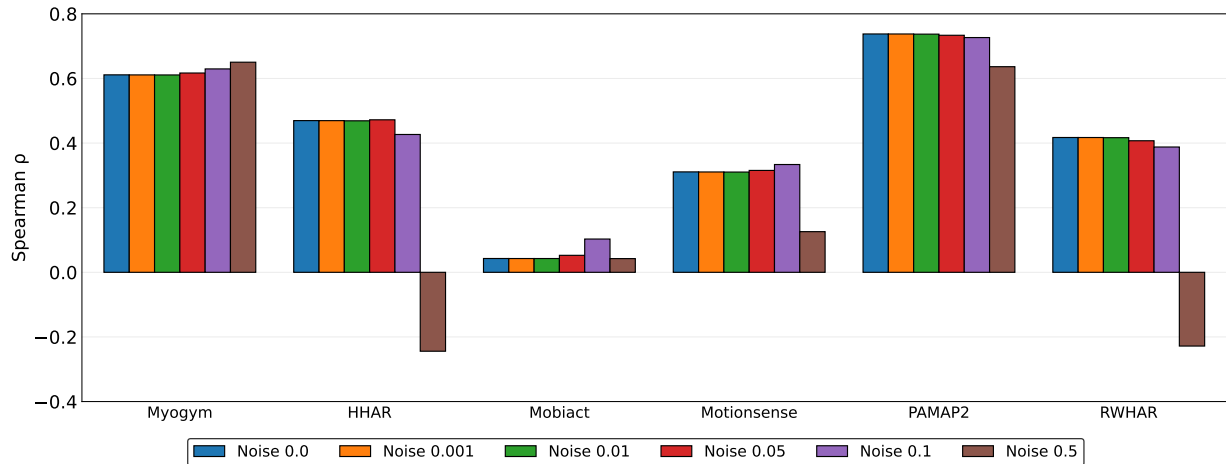


Fig. 5: Impact of data noise on ZCP: increasing the variance of the Gaussian noise has limited impact on the correlation.

for details). It performs comparably if not better, and can be utilized in situations where the optimal ZCP is not known beforehand.

In Fig. 2 (bottom), we extend the evaluation to the top 10 predicted architectures (as opposed to only the top-ranked one), ranking them by their validation F1-scores. We then quantify the gap between the overall best model and the best model identified within this top-10 subset, which we denote by Δ_{10} . We observe that *the best ZCPs have $\Delta_{10} < 1\%$* , demonstrating that training just the top 10 predicted architectures is sufficient to match the performance obtained after full scale training of 1500 networks.

To construct our random architecture search baseline, we randomly sample an architecture 1000 times and plot the mean of the test set F1-scores in light blue in Fig. 2, with the error bar representing the standard deviation. Broadly, random search achieves lower mean performance than ZCPs, but exhibits substantial variance. This suggests that while random search can occasionally yield lower Δ_1 , the substantial variance makes it an undesirable strategy for real-world settings where training runs are costly and time-consuming. This is also applicable when we randomly sample 10 architectures instead of just one. In contrast, the performance of ZCPs is consistent and reliable, making them attractive.

On the whole, with the use of ZCP, *we can train just 10 networks and obtain performance within 1-2% of full-scale training of 1500 architectures*. This reduces the computational effort by two orders of magnitude, making it highly useful from a practical standpoint.

B. Talent Rates of ZCPs

Next, we examine the talent rates of the ZCPs, i.e., the overlap between top 10% of models identified through ZCP and those obtained after full training (based on the validation F1-score). High talent rate ensures that, broadly, high performing models are discovered, even if the top predicted model has high Δ_1 . In such a case, instead of only training the top candidate architecture, top- k can be trained, where k can be a reasonable

number, e.g., 10%. After training, the model with the highest validation F1-score is chosen. This would provide a higher chance for successfully finding high performance networks.

Fig. 3 plots the talent rates of the ZCP measures. The multi-sensor datasets (PAMAP2 and RWHAR) and Myogym have higher talent rates, around 20%. Remaining single-sensor datasets like HHAR, Mobiact, and Myogym have lower talent rates, typically below 10%. Once again, the ensemble is comparable or better than individual ZCPs.

Similar to Section V-A, we compute the talent rate for random search using 10%, i.e., 150 architectures. For Myogym, RWHAR, Motionsense, and PAMAP2, the talent rate of ZCPs is comparable or higher than random search. This demonstrates the capability of ZCPs to broadly discover high performance architectures.

We perform full training with the top-10% of models predicted by ZCPs and denote the difference in performance to the top model as $\Delta_{10\%}$. We observe that $\Delta_{10\%} < \Delta_1$ overall and most ZCP produce $\Delta_{10\%} < 1\%$. Similar to Fig. 2, the random search can also be effective, but also suffers from substantial variance.

C. Spearman Rank Correlation

Here, we evaluate the ability of ZCPs to predict and rank network performance. We take all 1500 architectures, rank them based on the ZCPs, and compute Spearman rank correlation to fully trained models ordered by the validation F1-score. Higher correlation indicates better overall ability for predicting network performance.

Fig. 4 visualizes the Spearman rank correlations of the ZCPs across HAR datasets. For Myogym, PAMAP2, RWHAR, and HHAR, most ZCP measures achieve correlation of around 0.5. This indicates that ZCP are able to reliably rank network performance for these HAR datasets. Correspondingly, we observe in Fig. 2 that Δ_1 is low for these datasets.

Motionsense has lower correlation, but also low Δ_1 . Consequently, correlation alone does not imply low Δ_1 , which is the core metric of performance. Interestingly, Mobiact shows

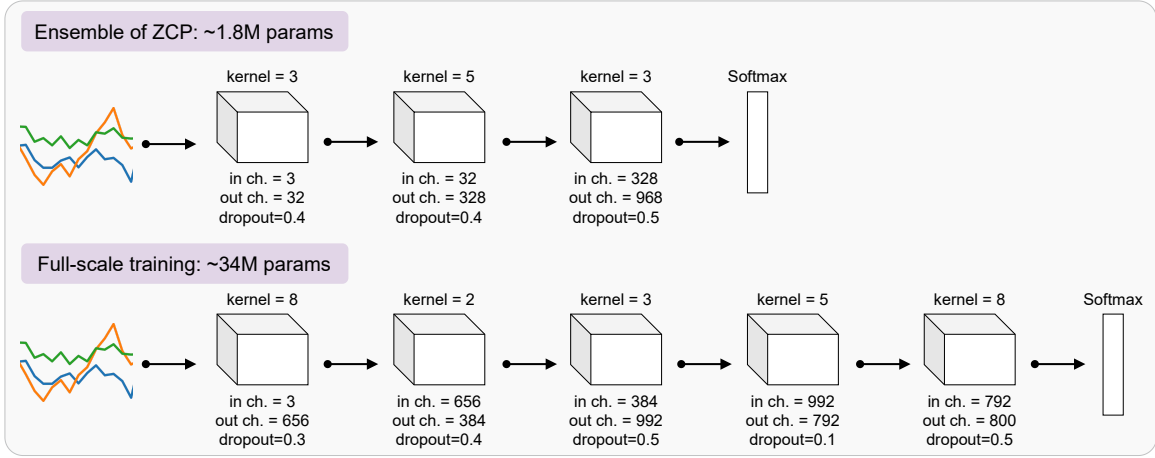


Fig. 6: Visualizing the best predicted architecture using the ensemble of ZCPs as well as best model obtained using full scale training for the Mobiact dataset. Each block in the figure comprises a 1D convolution layer, followed by ReLU activation and dropout. The ensemble identifies shallower architectures, with fewer trainable parameters.

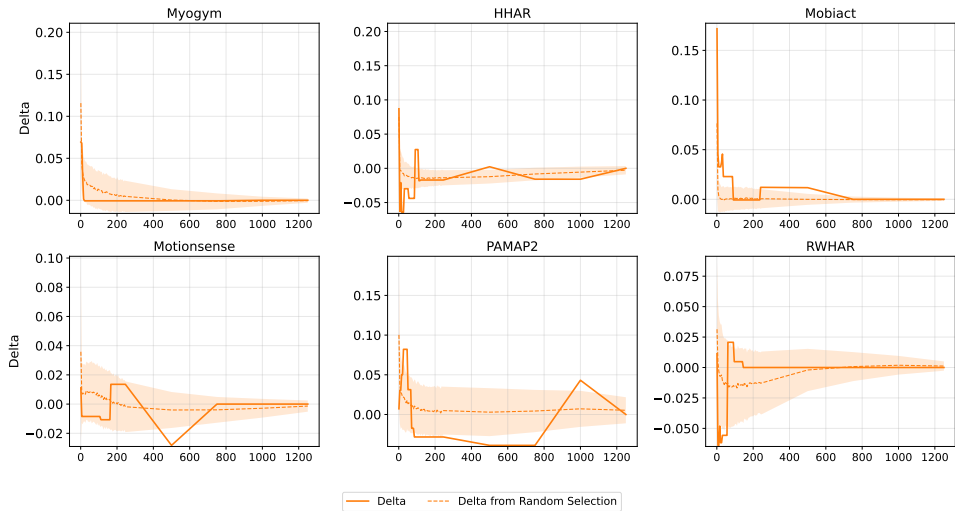


Fig. 7: Comparing the performance of ZCPs against random search.

low negative correlation, with only `synflow` obtaining high positive correlation and low Δ_1 . This demonstrates the value of data-agnostic ZCPs. In contrast to [5], [18], we find that the rank correlation alone is not the best indicator of ZCP performance, and must be coupled with other metrics such as Δ_1 and Δ_{10} to get a better picture of performance.

VI. DISCUSSION

Here, we first investigate the robustness of ZCP against data noise encountered during deployments. Subsequently, we visualize the top architectures discovered by the ensemble of ZCPs and full scale training. Finally, we compare ZCPs to random search by increasing the number of sampled architectures.

A. Impact of Data Noise

Often, wearable systems deployed in real-world scenarios are exposed to noisy conditions, whereas training data can

be from clean, laboratory settings. As such, robustness to noise during deployment is useful from a practical standpoint. We simulate data noise by adding Gaussian noise with zero mean and increasing variance $\in (0.0, 0.001, 0.01, 0.05, 0.5)$ to the test data alone. Subsequently, we compute the Spearman correlation between test performance of the 1500 networks in noisy conditions, against the architectures ranked by the ZCPs.

In Fig. 5, we observe that correlation remains consistent with the addition of Gaussian noise. Motionsense, HHAR, RWHAR, and PAMAP2 see a reduction in correlation only when the variance is high, at 0.5. This demonstrates that the ZCPs are robust to data noise, and can be employed to identify high performance models for practical, noisy scenarios.

B. Examining the Best Performing Architectures

Beyond metrics such as Δ_1 , Δ_{10} , talent rate, and Spearman's correlation, we also perform an examination of the architec-

tures discovered by the ZCPs as well as the best network obtained after full-scale training. In Fig. 6, we visualize both architectures for Mobiact only for brevity. Each block contains a 1D convolution layer, followed by ReLU activation [21] and dropout [22]. The kernel size, input and output channel sizes, and the dropout probability are also detailed in the figure.

We observe that the architecture identified by the ensemble of ZCPs contains three convolutional blocks. The kernel sizes are (3, 5, 3), the number of filters is (32, 328, 328), and dropout is (0.4, 0.4, 0.4). In contrast, the best performing model obtained via full scale training comprises five convolutional blocks, and kernel sizes are (8, 2, 3, 5, 8), number of filters is (656, 384, 992, 792, 800), and dropout is (0.3, 0.4, 0.5, 0.1, 0.5). The ensemble has a *shallow architecture* and lower number of filters across convolutional blocks. Accordingly, the *number of parameters is also lower*. This is more suitable for sensor-based HAR as simpler architectures overfit less and are more preferable from a deployment standpoint. We observe a similar tendency of ZCPs favoring shallower architectures across all datasets.

C. ZCPs vs Random Search

Fig. 2 reveals that performing random search can yield comparable mean test performance, but the substantial variance makes it unattractive. In Fig. 7, we conduct deeper analysis, by extending the random search to include an increasing number of sampled architectures. As before, we perform 1000 sampling trials, and compare the results against the ensemble of ZCPs.

For Myogym, HHAR, RWHAR, and Motionsense, ZCPs have lower delta than random search when the number of sampled architectures is below 100. However, the variance remains considerable for datasets such as Myogym, Motionsense, PAMAP2 and RWHAR, highlighting the advantage of utilizing ZCPs over random search.

VII. CONCLUSION

In this paper, we introduced Zero Cost Proxies to sensor-based HAR and evaluated their potential for identifying effective network architectures. First, we compared the performance between the best architectures predicted by the ZCPs against full scale training. We observed that the difference is surprisingly low, at around 5% when the top model is chosen, and around 1-2% when the top-10 models are trained. Subsequently, we investigated the talent rate, i.e., the overlap between high performing models identified through ZCPs and via full training. We also evaluated the Spearman rank correlation of ZCP ranked architectures and obtained higher correlations for HHAR, PAMAP2 and Myogym. Finally, we visualized performing architectures for Mobiact and discovered that ZCPs favor shallower, simpler architectures, indicating their practical utility. Overall, the integration of ZCPs into HAR pipelines and other wearable applications can result in reduced computational costs, highlighting their usability.

REFERENCES

- [1] A. Stisen, H. Blunck, S. Bhattacharya, T. S. Prentow, M. B. Kjærgaard, A. Dey, T. Sonne, and M. M. Jensen, “Smart devices are different: Assessing and mitigating mobile sensing heterogeneities for activity recognition,” in *Proceedings of the 13th ACM conference on embedded networked sensor systems*, 2015, pp. 127–140.
- [2] K. Yu, C. Sculio, M. Jaggi, C. Musat, and M. Salzmann, “Evaluating the search phase of neural architecture search,” *arXiv preprint arXiv:1902.08142*, 2019.
- [3] G. Bender, P.-J. Kindermans, B. Zoph, V. Vasudevan, and Q. Le, “Understanding and simplifying one-shot architecture search,” in *International conference on machine learning*. PMLR, 2018, pp. 550–559.
- [4] H. Liu, K. Simonyan, and Y. Yang, “Darts: Differentiable architecture search,” *arXiv preprint arXiv:1806.09055*, 2018.
- [5] M. S. Abdelfattah, A. Mehrotra, Ł. Dudziak, and N. D. Lane, “Zero-cost proxies for lightweight nas,” *arXiv preprint arXiv:2101.08134*, 2021.
- [6] A. Krizhevsky, G. Hinton *et al.*, “Learning multiple layers of features from tiny images,” 2009.
- [7] J. Deng, W. Dong, R. Socher, L.-J. Li, K. Li, and L. Fei-Fei, “Imagenet: A large-scale hierarchical image database,” in *2009 IEEE conference on computer vision and pattern recognition*. Ieee, 2009, pp. 248–255.
- [8] L. Li and A. Talwalkar, “Random search and reproducibility for neural architecture search,” in *Uncertainty in artificial intelligence*. PMLR, 2020, pp. 367–377.
- [9] B. Zoph and Q. V. Le, “Neural architecture search with reinforcement learning,” *arXiv preprint arXiv:1611.01578*, 2016.
- [10] H. Rakhshani, H. I. Fawaz, L. Idoumghar, G. Forestier, J. Lepagnot, J. Weber, M. Brévilliers, and P.-A. Muller, “Neural architecture search for time series classification,” in *2020 International Joint Conference on Neural Networks (IJCNN)*. IEEE, 2020, pp. 1–8.
- [11] L. Pellatt and D. Roggen, “Fast deep neural architecture search for wearable activity recognition by early prediction of converged performance,” in *Proceedings of the 2021 ACM International Symposium on Wearable Computers*, 2021, pp. 1–6.
- [12] X. Wang, X. Wang, T. Lv, L. Jin, and M. He, “HARNAS: Human Activity Recognition Based on Automatic Neural Architecture Search Using Evolutionary Algorithms,” *Sensors (Basel, Switzerland)*, vol. 21, no. 20, p. 6927, 2021. [Online]. Available: <https://www.mdpi.com/1424-8220/21/20/6927>
- [13] W. N. Ismail, H. A. Alsalamah, M. M. Hassan, and E. Mohamed, “Auto-har: An adaptive human activity recognition framework using an automated cnn architecture design,” *Heliyon*, vol. 9, no. 2, 2023.
- [14] Y. Zhou, T. King, Y. Huang, H. Zhao, T. Riedel, T. Röddiger, and M. Beigl, “Enhancing efficiency in har models: Nas meets pruning,” in *2024 IEEE International Conference on Pervasive Computing and Communications Workshops and other Affiliated Events (PerCom Workshops)*, 2024, pp. 33–38.
- [15] R. Chavarriaga, H. Saghaf, A. Calatroni, S. T. Digumar, G. Tröster, J. d. R. Millán, and D. Roggen, “The opportunity challenge: A benchmark database for on-body sensor-based activity recognition,” *Pattern Recognition Letters*, vol. 34, no. 15, pp. 2033–2042, 2013.
- [16] E. Liberis, Ł. Dudziak, and N. D. Lane, “unas: Constrained neural architecture search for microcontrollers,” in *Proceedings of the 1st Workshop on Machine Learning and Systems*, 2021, pp. 70–79.
- [17] T. King, Y. Zhou, T. Röddiger, and M. Beigl, “Micronas for memory and latency constrained hardware aware neural architecture search in time series classification on microcontrollers,” *Scientific Reports*, vol. 15, no. 1, p. 7575, 2025.
- [18] J. C. Mellor, J. Turner, A. J. Storkey, and E. J. Crowley, “Neural architecture search without training,” *CoRR*, vol. abs/2006.04647, 2020. [Online]. Available: <https://arxiv.org/abs/2006.04647>
- [19] A. Krishnakumar, C. White, A. Zela, R. Tu, M. Safari, and F. Hutter, “Nas-bench-suite-zero: Accelerating research on zero cost proxies,” 2022. [Online]. Available: <https://arxiv.org/abs/2210.03230>
- [20] J. Lukasik, M. Moeller, and M. Keuper, “An evaluation of zero-cost proxies – from neural architecture performance to model robustness,” 2023. [Online]. Available: <https://arxiv.org/abs/2307.09365>
- [21] V. Nair and G. E. Hinton, “Rectified linear units improve restricted boltzmann machines,” in *Proceedings of the 27th international conference on machine learning (ICML-10)*, 2010, pp. 807–814.
- [22] N. Srivastava, G. Hinton, A. Krizhevsky, I. Sutskever, and R. Salakhutdinov, “Dropout: a simple way to prevent neural networks from overfitting,”

The journal of machine learning research, vol. 15, no. 1, pp. 1929–1958, 2014.

- [23] J. Frankle and M. Carbin, “The lottery ticket hypothesis: Finding sparse, trainable neural networks,” in *International Conference on Learning Representations*, 2019. [Online]. Available: <https://openreview.net/forum?id=rJl-b3RcF7>
- [24] N. Lee, T. Ajanthan, and P. H. S. Torr, “SNIP: single-shot network pruning based on connection sensitivity,” *CoRR*, vol. abs/1810.02340, 2018. [Online]. Available: <http://arxiv.org/abs/1810.02340>
- [25] C. Wang, G. Zhang, and R. B. Grosse, “Picking winning tickets before training by preserving gradient flow,” *CoRR*, vol. abs/2002.07376, 2020. [Online]. Available: <https://arxiv.org/abs/2002.07376>
- [26] H. Tanaka, D. Kunin, D. L. K. Yamins, and S. Ganguli, “Pruning neural networks without any data by iteratively conserving synaptic flow,” *CoRR*, vol. abs/2006.05467, 2020. [Online]. Available: <https://arxiv.org/abs/2006.05467>
- [27] J. Turner, E. J. Crowley, G. Gray, A. J. Storkey, and M. F. P. O’Boyle, “Blockswap: Fisher-guided block substitution for network compression,” *CoRR*, vol. abs/1906.04113, 2019. [Online]. Available: <http://arxiv.org/abs/1906.04113>
- [28] C. Chatzaki, M. Pediaditis, G. Vavoulas, and M. Tsiknakis, “Human daily activity and fall recognition using a smartphone’s acceleration sensor,” in *International Conference on Information and Communication Technologies for Ageing Well and e-Health*. Springer, 2016, pp. 100–118.
- [29] M. Malekzadeh, R. G. Clegg, A. Cavallaro, and H. Haddadi, “Protecting sensory data against sensitive inferences,” in *Proceedings of the 1st Workshop on Privacy by Design in Distributed Systems*, 2018, pp. 1–6.
- [30] H. Koskimäki, P. Siirtola, and J. Röning, “Myogym: introducing an open gym data set for activity recognition collected using myo armband,” in *Proceedings of the 2017 ACM International Joint Conference on Pervasive and Ubiquitous Computing and Proceedings of the 2017 ACM International Symposium on Wearable Computers*, 2017, pp. 537–546.
- [31] A. Reiss and D. Stricker, “Introducing a new benchmarked dataset for activity monitoring,” in *2012 16th international symposium on wearable computers*. IEEE, 2012, pp. 108–109.
- [32] T. Szttyler and H. Stuckenschmidt, “On-body localization of wearable devices: An investigation of position-aware activity recognition,” in *2016 IEEE international conference on pervasive computing and communications (PerCom)*. IEEE, 2016, pp. 1–9.
- [33] D. P. Kingma, “Adam: A method for stochastic optimization,” *arXiv preprint arXiv:1412.6980*, 2014.
- [34] H. Haresamudram, I. Essa, and T. Plötz, “Assessing the state of self-supervised human activity recognition using wearables,” *Proceedings of the ACM on Interactive, Mobile, Wearable and Ubiquitous Technologies*, vol. 6, no. 3, pp. 1–47, 2022.
- [35] T. Plötz, “Applying machine learning for sensor data analysis in interactive systems: Common pitfalls of pragmatic use and ways to avoid them,” *ACM Computing Surveys (CSUR)*, vol. 54, no. 6, pp. 1–25, 2021.